High-Power Microwave Amplifier Using an Antiparallel Avalanche-Diode Pair

HIROHISA KAWAMOTO, MEMBER, IEEE

Abstract—**Two high-efficiency avalanche diodes, each placed in opposite polarity to the other at the ends of an approximately one-half wavelength transmission line, have worked as a high-power reflection-type amplifier. The circuit configuration is called an antiparallel pair of high-efficiency avalanche diodes. The antiparallel amplifier has provided 200-W pulsed output power with a 10-dB gain at 1.01 GHz.**

I. Introduction

Amplification with high-efficiency avalanche diodes [1] was first reported in 1967 by Prager, Chang, and Weisbrod [2]. This was followed by papers from several authors [3]–[7] who also worked on high-efficiency diodes, while others [8]–[11] reported on related self-pumped parametric amplifiers.

This paper describes a new reflection-type amplifier composed of two physically separated high-efficiency avalanche diodes. Each diode is placed in opposite polarity to the other at the ends of an essentially one-half wavelength transmission line. This configuration is called an antiparallel pair of high-efficiency avalanche diodes, and was reported earlier by the author and his colleague to work as an oscillator [12], [13]. The antiparallel amplifier described here has delivered pulsed output power of 200 W at 1.01 GHz with a power gain of 10 dB.

II. Mechanism of Amplification

Fig. 1 is a schematic circuit diagram of the antiparallel amplifier. The two avalanche diodes are both reverse-biased. An input–output transmission line is connected to the midpoint 0 between the two diodes as shown in Fig. 1. A low-pass filter is placed in the input–output line, one-quarter wavelength from the midpoint. A circulator is placed in the input–output line next to the low-pass filter.

Schematic RF signal waveforms within the antiparallel amplifier circuit, shown in Fig. 2, qualitatively explain the mechanism of amplification. The arrows in Fig. 2 indicate only those wave-traveling directions that are important in understanding the mechanism. A positive half-sine wave A_i of the input signal travels through

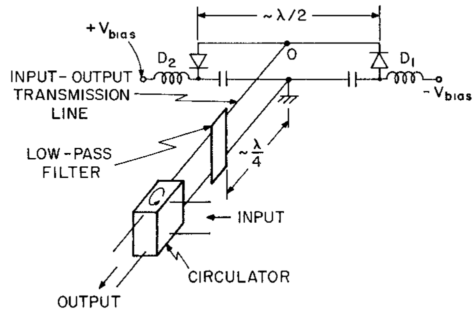

Fig. 1. Schematic diagram of reflection-type amplifier using antiparallel avalanche-diode pair.

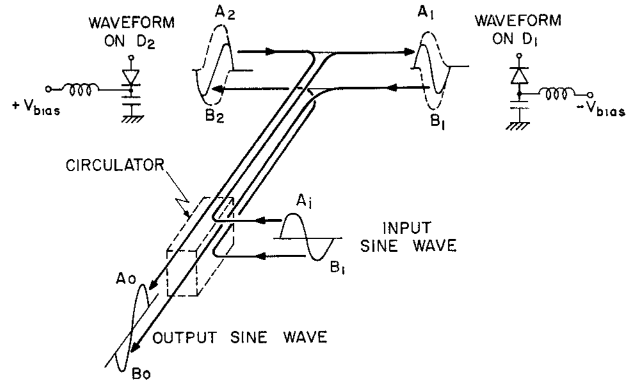

Fig. 2. RF waveforms inside antiparallel amplifier illustrating mechanism of amplification.

the midpoint to the diode D_1.[1] A dotted waveform A_1 shows the positive half-sine wave incident to D_1. The positive voltage A_1 causes the diode voltage to exceed the breakdown voltage, and as a result of trapped-plasma formation [14], [15] induces a negative half-sine wave on the diode. A dotted waveform B_1 shows the generated negative half-sine wave. The resultant waveform on D_1 is the sum of A_1 and B_1, which is shown by a solid waveform in Fig. 2. The start of B_1 is delayed by about 100 ps from the start of A_1 [13], [16]; therefore, the resultant waveform exhibits the leading edge of A_1 followed by the trailing edge of B_1. A portion of the generated wave B_1 travels through the midpoint to the

Manuscript received May 5, 1971; revised July 15, 1971. This work was supported by the U. S. Air Force Avionics Laboratory, Wright-Patterson AFB, Ohio, under Air Force Contract F33615-70-C-1725.

The author is with the RCA Laboratories, Princeton, N. J. 08540.

[1] The positive wave that travels toward D_2 is not shown in Fig. 2; since it does not activate D_2, it is not important in understanding the mechanism. The negative wave that travels toward D_1 is not shown either for the same reason.

output terminal, and forms a negative half-sine wave B_o of the output signal. The distance between the diodes and the midpoint is so adjusted that a round trip from the midpoint to the diode equals one half-cycle of the input signal. A negative half-sine wave B_i of the input signal, therefore, arrives at the midpoint just when the negative wave B_1 arrives at the midpoint from the diode D_1. The signal B_i combined with a portion of B_1 forms a negative half-sine wave B_2 and travels to the diode D_2. D_2 is placed in opposite polarity with respect to D_1. The negative B_2 induces a positive half-sine wave A_2 on the diode D_2, in the same manner that a positive half-sine wave has induced a negative half-sine wave on the diode D_1. The resultant waveform on D_2 is shown by a solid line in Fig. 2. A_2 travels to the output terminal through the midpoint and forms a positive half-sine wave A_o of the output signal. The next A_i of the input signal arrives at the midpoint just when A_2 arrives at the midpoint. A_i combined with a portion of A_2 forms the positive half-sine wave A_1 and travels to the diode D_1. A_1 induces the negative half-sine wave B_1 of the next cycle, a portion of which travels to the output terminal and forms a negative half-sine wave B_o of the output signal. The antiparallel pair acts as an amplifier when the amplitude of B_o and A_o is higher than that of A_i and B_i, or equivalently when the amplitude of B_1 and A_2 is higher than that of A_1 and B_2. This condition is satisfied when proper incident waveform and bias voltage are applied to each diode.

The relationship between the physical separation L of the two diodes and the wavelength λ of the amplified signal is derived from the condition that a round-trip time from the midpoint to the diode equals one half-cycle of the input signal:

$$L/V_p + \tau_d = \lambda/2V_p \tag{1}$$

where V_p is the phase velocity and τ_d the response delay time between the incident and the generated half-sine wave [13], [16]. Equation (1) has been used to calculate the frequency of oscillation for the antiparallel oscillator [13].

III. Waveform Measurements

RF-voltage waveforms measured on the antiparallel circuit in the amplifier mode further demonstrate the mechanism of amplification described in Section II. The waveforms have been measured with a 1000-Ω microwave chip resistor (two 500-Ω resistors in series) and a Tektronix-type 661 sampling oscilloscope having a 90-ps rise time. The waveform at the cathode of D_1 (top of Fig. 3) exhibits the leading edge of the positive wave incident to D_1 followed by the trailing edge of the negative wave generated inside D_1. The waveform at the anode of D_2 (bottom of Fig. 3) exhibits the leading edge of the negative wave incident to D_2 and the trailing edge of the positive wave generated inside D_2. The waveform measured represents an RF component of the diode voltage since the waveform is measured across the diode in series with the bypass capacitor (Fig. 2). The averaged autobias across each diode is approximately 105 V. The output power of the amplifier has been reduced when measuring the waveforms, since the two resistors load the circuit. The waveforms in Fig. 3 were taken with a test setup in which the amplifier delivered 150-W output power with 20-W input power. The waveforms at D_1 and D_2 repeat themselves with a period of 1 ns—corresponding to the operating frequency of 1 GHz. The phase relationship between the two waveforms has been determined by operating the sampling scope in a dual-trace mode. The two pictures in Fig. 3 exhibit the phase relationship. The positive wave incident to D_1 is delayed by 0.5 ns from the negative wave incident to D_2; the wave incident to D_1 is 180° out of phase with respect to the wave incident to D_2. Therefore, the mechanism of amplification may be simplified as follows. The diode D_1 amplifies the positive half-sine wave of the 1-GHz input and the diode D_2 amplifies the negative half-sine wave of the input. The mechanism for the antiparallel amplifier is similar to that for a conventional transistor push–pull amplifier, in which one of the two transistors amplifies one half-cycle of the input signal, and the other amplifies another half-cycle of the input signal. It should be noted, however, that they are not completely equivalent. The two transistors in the push–pull amplifier are relatively independent in operation from each other, e.g., the push–pull circuit with one of the transistors missing still works as an amplifier even though the output waveform is distorted. The two diodes in the antiparallel amplifier, however, are closely coupled to each other as seen from the previous discussions. The antiparallel circuit would not operate as an amplifier with only one diode.

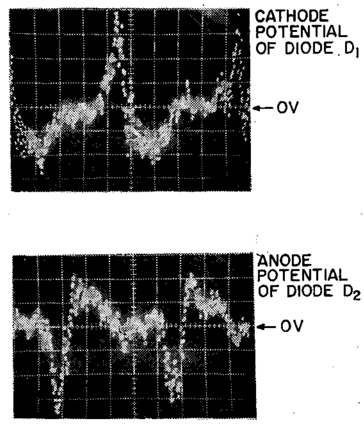

Fig. 3. Sampling-oscilloscope voltage waveforms on diodes in antiparallel amplifier. Input power is 20 W and output power is 150 W. Vertical scale: 33.2 V/div; horizontal scale: 200 ps/div.

Fig. 4 shows a waveform at the midpoint between the diodes. The waveform has been measured by connecting a 1000-Ω microwave resistor to the midpoint. The output power of the amplifier has been reduced to 110 W, with an input power of 20 W.

It should be noted that the waveform is very nonsinusoidal at the diode positions but almost sinusoidal

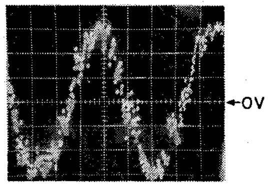

Fig. 4. Almost sinusoidal waveform at midpoint between two diodes forming antiparallel pair. Input power is 20 W and output power is 110 W. Vertical scale: 66.4 V/div; horizontal scale: 200 ps/div.

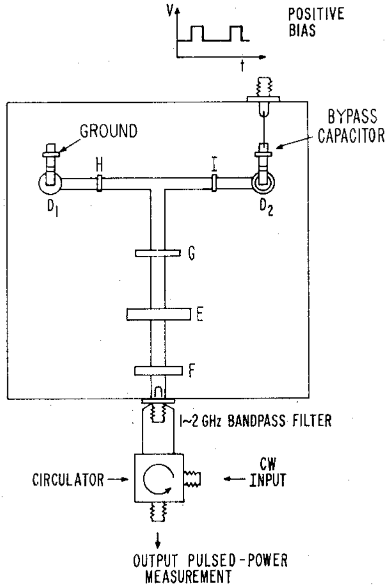

Fig. 5. Antiparallel amplifier on a T-shaped microstrip-line circuit.

at the midpoint. This is because the positive and negative half-sine waves arrive alternatively at the midpoint every 500 ps, thus producing an almost sinusoidal waveform. The waveform measurements indicate that the signal at the midpoint is low on harmonic content even though the signals at the diodes are high on harmonic content. The fundamental and harmonic signals within the circuit have been probed by using a small electric-field probe [12]. As has been found for the antiparallel oscillator circuit [12], the probe measurements have verified that both the second and the third harmonic are strong at the diode positions but very weak at the midpoint. The second and third harmonic signals have also been found to be very weak along the output line. This is because the wave traveling toward the load on the output line is the fundamental sine wave formed at the midpoint, and the wave traveling toward the midpoint is also the sine wave from the input terminal combined with the sine wave reflected at the low-pass filter.

IV. Amplifier Experiment

The antiparallel amplifier experiment has been performed using a T-shaped 50-Ω microstrip-line circuit as shown in Fig. 5. The circuit is made of the conventional microstrip of metal on Teflon. The distance between the two diodes is 8.3 cm. The substrate has a dielectric constant of 2.3. A small copper chip is used to ground the p-side of D_1. The bias voltage is applied to the diode D_2 through a thin inductive wire. A 100-pF bypass capacitor is placed between D_2 and the ground plane. The bias circuit of Fig. 5, which has only one power source, is slightly different from that of Fig. 1, which has two sources. An AIL-type 125 power oscillator supplies a CW input power to the circulator. The diodes are pulse-operated. The bias voltage is a pulse voltage superimposed on a dc bias. The diodes would have been burned out without the dc bias, because the diodes would have a low impedance during their inactive period and would absorb the high-power input signal. With the dc bias, the diodes have a very high impedance during the off period and reflect the input RF power. The input power is monitored with a directional coupler and an HP341B power meter. The pulsed RF output is measured with precision attenuators and a calibrated HP423A crystal detector. Fig. 6 gives an experimental setup of the amplifier, and also exhibits the two chip resistors connected to D_2 used for the sampling-oscilloscope waveform measurements.

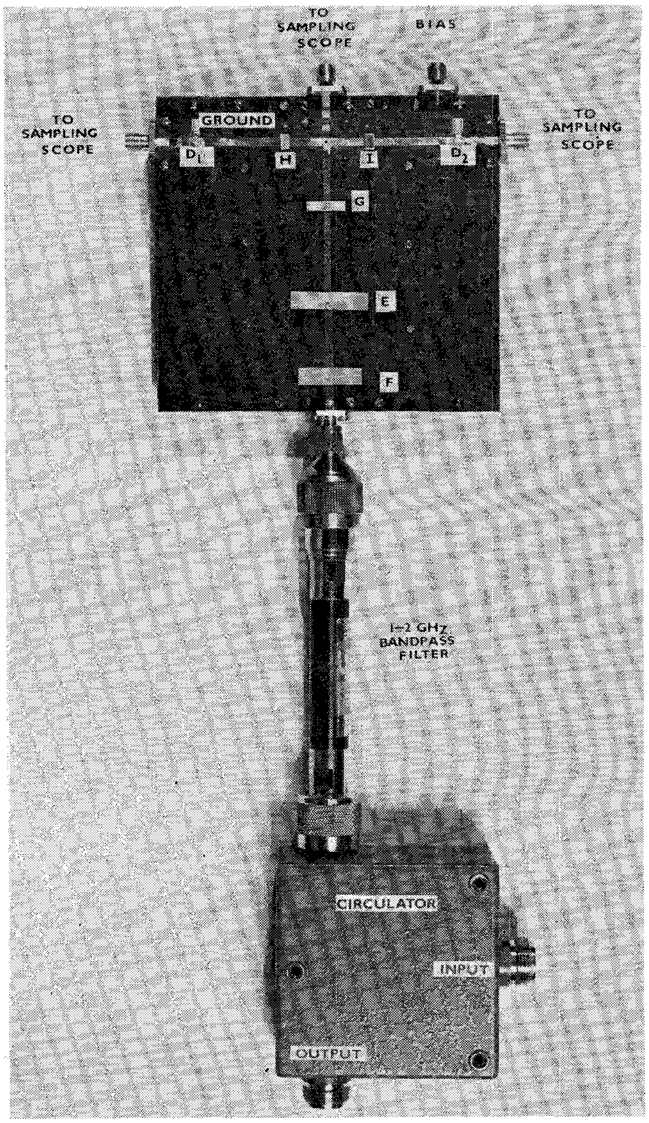

Fig. 6. Antiparallel microstrip amplifier.

The thin gold-plated steel plates E and F are the main tuning elements that act as a low-pass filter[2] [17]. The fine tuning elements G, H, and I have been found to be very useful in maximizing the amplifier gain and output power. A 1.0- to 2.0-GHz bandpass filter is used to block the dc signal as well as to ensure a single frequency in the power measurements. A circulator is placed next to the bandpass filter.

The admittance looking from the midpoint toward the output circuit loaded with a 50-Ω resistor has been measured by using an HP8410A network analyzer. The line connecting the two diodes has been disconnected at the midpoint. A 50-Ω coaxial line has been connected to the midpoint from the back side of the circuit during the measurement. The measured admittance is $(6.78+j\,8.64)$ mmho at 1.01 GHz. The output power has been calculated from

$$P_o = V_p^2/2G \tag{2}$$

where V_p is the amplitude of the sine wave at the midpoint obtained from waveform measurement (Fig. 4) and G the real part of the admittance. P_o is calculated to be 116 W, which is in good agreement with the measured output power of 110 W.

The diodes have a p-n-n$^+$ tapered-cylinder structure [18]. The diameter of the diodes is approximately 0.020 in. The junction was formed by boron diffusion into n-type silicon epitaxial wafers. The resistivity of the epitaxial layer is around 6 Ω·cm. The breakdown voltage of the diodes is about 150 V and the punch-through voltage is 27 V.

The circuit operates as either an amplifier or an oscillator, depending upon the number, sizes, and positions of the tuning elements. The amplifier tends to be a saturation-type amplifier rather than a linear amplifier, although it does have a short linear portion in the input–output characteristics.

The detected output RF envelope and the pulsed diode current shown in Fig. 6 were observed with such a saturation-type amplifier which has a very nonlinear input–output characteristic. Fig. 7(a) shows a saturated output power of 200 W with a 20-W input power. The power conversion efficiency, which is RF output divided by dc input plus RF input, is 16.7 percent. The output envelope during the off period represents a reflection of the input power by the diodes. The width of the current pulse determines the width of the output RF envelope. Fig. 7(b) was taken when there was no input power to the amplifier. The CW input has also been replaced by a pulsed input whose width is shorter than the bias width. The pulsewidth of the output RF envelope has followed that of the input RF envelope. For this reason, it has been concluded that the circuit is not a triggered oscillator but an amplifier.

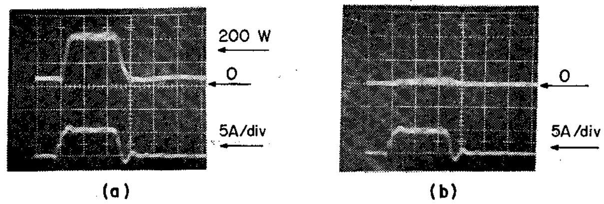

Fig. 7. Detected RF output (top) and diode current (bottom). (a) With a 20-W CW input. (b) Without input.

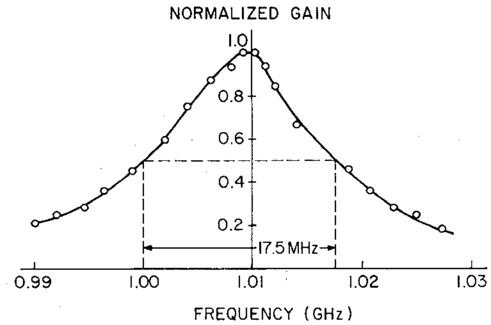

Fig. 8. Gain versus frequency characteristics of saturation-type antiparallel amplifier.

The tuning elements of the amplifier have also been adjusted to obtain the maximum linear range in its input–output characteristics. The amplifier has a residual output of 7 W. The linear portion is from 30 W to 200 W. The output power saturates at 200 W with a 10-dB power gain. The detected RF envelope is clean at the saturated level. However, it is noisy at low levels as previously reported [4]. Fig. 8 shows the gain versus frequency characteristics of the saturation-type amplifier. The 3-dB bandwidth is 17.5 MHz with a 1.01-GHz center frequency of amplification. The center frequency is equal to the frequency of oscillation when the circuit is tuned as an oscillator.

V. Discussion

It has been observed that the antiparallel amplifier is a balanced amplifier and has low harmonic content in the output line. The nature of low harmonic content seems to make the antiparallel configuration more suitable for amplifier applications than a single-diode circuit [2]–[7]. The single-diode circuit has high harmonic content [7], [17]. The harmonic signals leaking out of the low-pass filter may reflect at the circulator and may cause difficulties in tuning the amplifier. With low harmonic content, the antiparallel circuit has negligible higher harmonics arriving at the circulator. The circuit,

[2] The main function of the low-pass filter in this circuit is to adjust the amount of reflection or transmission for the fundamental-frequency signal so that the diodes are most effectively triggered into power generation with a minimum of input power. The low-pass filter also reflects all the harmonic signals coming from the midpoint, even though those harmonic signals are weak, as seen in Section III.

therefore, is free from the disturbances caused by the reflected harmonic signals.

This experiment, as well as others [2], [4], [7], suggests that the high-power amplifier with high-efficiency avalanche diodes can best be used as a saturation-type amplifier which has a very nonlinear, or threshold-type, input–output characteristic. The threshold nature of the input–output characteristics is believed to originate from a triggering-type response of the diode. To initiate the trapped plasma, the incident wave to the diode must satisfy two conditions: 1) the amplitude of the incident wave plus the diode bias voltage must be sufficiently higher than the breakdown voltage [19]; and 2) the leading edge of the incident wave must be sharp enough to launch the traveling avalanche zone [14], [16]. These requirements for the incident wave contribute to the existence of a threshold level for RF input to activate the diode.

VI. Conclusions

It has been demonstrated that an antiparallel diode pair, spaced approximately one-half wavelength apart, works as a high-power reflection-type amplifier. The amplifier is of a saturation type. Waveform measurements indicate that the operation of the amplifier can be explained in terms of an incident wave triggering the trapped plasma within the diode and a reflected wave delivering amplified power to the load. The antiparallel circuit has very low harmonic content, which facilitates the circuit tuning as an amplifier. The amplifier has provided a 200-W output power with a 10-dB gain. The center frequency is 1.01 GHz with a 3-dB bandwidth of 17.5 MHz.

Acknowledgment

The author wishes to thank S. G. Liu for his comments on the manuscript and for supplying the diodes; E. L. Allen, Jr., for his technical assistance; K. K. N. Chang for his encouragement and support; and H. J. prager for critical reading of the manuscript.

References

[1] H. J. Prager, K. K. N. Chang, and S. Weisbrod, "High-power, high-efficiency silicon avalanche diodes at ultra high frequencies," *Proc. IEEE* (Lett.), vol. 55, Apr. 1967, pp. 586–587.

[2] ——, "Anomalous silicon avalanche diodes for microwave generations," presented at the 1967 Topic High Frequency Generation and Amplification, Cornell Univ., Ithaca, N. Y.

[3] G. Gibbons and M. I. Grace, "High-efficiency avalanche-diode oscillators and amplifiers in *X*-band," *Proc. IEEE* (Lett.), vol. 58, Mar. 1970, pp. 512–513.

[4] R. J. Hess and D. A. Floyd, "High-efficiency solid-state microwave amplifier using TRAPATT diodes," in *1970 IEEE Int. Microwave Symp. Dig.*

[5] H. J. Prager, K. K. N. Chang, and S. Weisbrod, "Power amplification with anomalous avalanche diodes," *IEEE Trans. Microwave Theory Tech.*, vol. MTT-18, Nov. 1970, pp. 956–963.

[6] W. J. Evans, "CW TRAPATT amplification," *IEEE Trans. Microwave Theory Tech.*, vol. MTT-18, Nov. 1970, pp. 986–988.

[7] S. G. Liu, H. J. Prager, K. K. N. Chang, J. J. Risko, and S. Weisbrod, "High-power harmonic-extraction and triggered-amplification with high-efficiency avalanche diode," in *1971 IEEE Int. Solid-State Circuits Conf. Dig.*, pp. 176–177.

[8] B. Hoefflinger, C. P. Snapp, and L. A. Stark, "High-efficiency avalanche resonance pumped amplification," in *1969 Int. Microwave Symp. Dig.*, pp. 255–260.

[9] M. I. Grace, "Parametrically generated high efficiency low frequency oscillations in avalanche diodes," *Electron. Lett.*, vol. 55, 1969, pp. 163–164.

[10] J. F. Dienst, R. V. D'Aiello, and E. E. Thomas, "Power amplification using an avalanche diode," *Electron. Lett.*, vol. 5, July 1969, pp. 308–309.

[11] J. M. Assour and R. V. D'Aiello, "Silicon avalanche diodes as oscillators and power amplifiers in *S*-band," in *1970 IEEE Int. Solid-State Circuits Conf. Dig.*, pp. 14–15, 180.

[12] H. Kawamoto, "Anti-parallel operation of four high-efficiency avalanche diodes," in *1971 IEEE Int. Solid-State Circuits Conf. Dig.*, pp. 178–179.

[13] H. Kawamoto and S. G. Liu, "Anti-parallel pair of high-efficiency avalanche diodes," *Proc. IEEE* (Lett.), vol. 59, Mar. 1971, pp. 427–428.

[14] A. S. Clorfeine, R. J. Ikola, and L. S. Napoli, "A theory for the high-efficiency mode of oscillation in avalanche diodes," *RCA Rev.*, vol. 30, Sept. 1969, pp. 397–421.

[15] B. C. DeLoach, Jr., and D. L. Scharfetter, "Device physics of TRAPATT oscillators," *IEEE Trans. Electron Devices*, vol. ED-17, Jan. 1970, pp. 9–21.

[16] H. Yanai, H. Torizuka, N. Yamada, and K. Ohkubo, "Experimental analysis for the large-amplitude high-efficiency mode of oscillation with Si avalanche diodes," *IEEE Trans. Electron Devices*, vol. ED-17, Dec. 1970, pp. 1067–1076.

[17] S. G. Liu, "Microstrip high-power high-efficiency avalanche-diode oscillator," *IEEE Trans. Microwave Theory Tech.*, vol. MTT-17, Dec. 1969, pp. 1068–1071.

[18] S. G. Liu and J. J. Risko, "Fabrication and performance of kilowatt *L*-band avalanche diodes," *RCA Rev.*, vol. 31, Mar. 1970, pp. 3–19.

[19] W. J. Evans, "Computer experiments on TRAPATT diodes," *IEEE Trans. Microwave Theory Tech.*, vol. MTT-18, Nov. 1970, pp. 862–871.